Relationships of trace gases and aerosols and the emission characteristics at Lin'an, a rural site in eastern China, during spring 2001

Tao Wang,[1] C. H. Wong,[1] T. F. Cheung,[1,2] D. R. Blake,[3] R. Arimoto,[4] K. Baumann,[5] J. Tang,[6] G. A. Ding,[6] X. M. Yu,[7] Y. S. Li,[1] D. G. Streets,[8] and I. J. Simpson[3]

Received 28 August 2003; revised 12 December 2003; accepted 9 January 2004; published 28 August 2004.

[1] We present measurements of trace gases and fine aerosols obtained from a rural site in eastern China during 18 February to 30 April 2001. The field program aimed to characterize the variations in aerosol and gaseous pollutant concentrations and the emission signatures from the inland region of eastern China in the spring season. The data included O_3, CO, NO, NO_y^*, SO_2, methane, C_2-C_8 nonmethane hydrocarbons (NMHCs), C_1-C_2 halocarbons, and the chemical composition of PM2.5. The average hourly mixing ratios (±standard deviation) of CO, SO_2, and NO_y^* were 677 (±315) ppbv, 15.9 (±14.6) ppbv, and 13.8 (±7.2) ppbv, respectively. The mean daytime ozone mixing ratio was 41 (±19) ppbv. The most abundant NMHC was ethane (3189 ± 717 pptv), followed by ethyne (2475 ± 1395 pptv), ethene (1679 ± 1455 pptv), and toluene (1529 ± 1608 pptv). Methyl chloride was the most abundant halocarbon (1108 ± 653 pptv). The average concentrations of particulate organic matter (POM, as organic carbon, OC, times 1.4) and elemental carbon (EC) in PM2.5 were 21.5 (±7) $\mu g/m^3$ and 2.5 (±0.7) $\mu g/m^3$, respectively, and sulfate and nitrate levels were 17.3 (±6.6) and 6.5 (±4) $\mu g/m^3$, respectively. CO showed moderate to good correlation with NO_y^* ($r^2 = 0.59$), OC ($r^2 = 0.65$), CH_3Cl ($r^2 = 0.59$), soluble potassium ($r^2 = 0.53$), and many NMHCs, indicating contributions from the burning of biofuel/biomass. CO also correlated with an industrial tracer, C_2Cl_4, indicative of some influence from industrial sources. SO_2, on the other hand, correlated well with EC ($r^2 = 0.56$), reflecting the contribution from the burning of coal. Ammonium was sufficiently abundant to fully neutralize sulfate and nitrate, indicating that there were strong emissions of ammonia from agricultural activities. Silicon and calcium had poor correlations with iron and aluminum, revealing the presence of source(s) for Si and Ca other than from soil. Examination of C_2H_2/CO, C_3H_8/C_2H_6, nitrate/(nitrate + NO_y^*), and sulfate/(SO_2 + sulfate) suggested that relatively fresh air masses had been sampled at the study site in the spring season. Comparison of the observed ratios/slopes with those derived from emission inventories showed that while the observed SO_2/NO_y^* ratio (1.29 ppbv/ppbv) in March was comparable (within 20%) to the inventory-derived ratio for the study region, the measured CO/NO_y^* slope (37 ppbv/ppbv) was about 200% larger. The observed slope of CO relative to NMHC (including ethane, propane, butanes, ethene, and ethyne) also indicated the presence of excess CO, compared to the ratios from the inventories. These results strongly suggest that emissions of CO in eastern China have been underrepresented. The findings of this study highlight the importance of characterizing trace gases and aerosols within source regions of the Asian continent. The springtime results were also compared with data previously collected at the site in 1999–2000 and with those obtained on the Transport and Chemical Evolution over the

[1]Department of Civil and Structural Engineering, Hong Kong Polytechnic University, Hong Kong, China.
[2]Now at Environment, Transport and Works Bureau, Hong Kong Special Administrative Region, Hong Kong, China.
[3]Department of Chemistry, University of California, Irvine, California, USA.
[4]Environmental Monitoring and Research Center, New Mexico State University, Carlsbad, New Mexico, USA.
[5]School of Earth and Atmospheric Sciences, Georgia Institute of Technology, Atlanta, Georgia, USA.
[6]Chinese Academy of Meteorological Sciences, Beijing, China.
[7]Lin'an Baseline Air Pollution Monitoring Station, Zhejiang, China.
[8]Decision and Information Sciences Division, Argonne National Laboratory, Argonne, Illinois, USA.

0148-0227/04/2003JD004119$09.00

Pacific (TRACE-P) aircraft and from a coastal site in South China for the same study period. *INDEX TERMS:* 0305 Atmospheric Composition and Structure: Aerosols and particles (0345, 4801); 0345 Atmospheric Composition and Structure: Pollution—urban and regional (0305); 0365 Atmospheric Composition and Structure: Troposphere—composition and chemistry; 0394 Atmospheric Composition and Structure: Instruments and techniques; *KEYWORDS:* trace gases and aerosols, emission patterns, rural eastern China

Citation: Wang, T., et al. (2004), Relationships of trace gases and aerosols and the emission characteristics at Lin'an, a rural site in eastern China, during spring 2001, *J. Geophys. Res.*, *109*, D19S05, doi:10.1029/2003JD004119.

1. Introduction

[2] Rapid industrialization in China has stimulated scientific research on possible impacts of the increasing emissions of gases and aerosols on the atmospheric environment and various ecosystems. The emissions of air pollutants have been linked to region-wide pollution such as acid deposition [e.g., *Wang and Wang*, 1995], photochemical ozone [e.g., *Luo et al.*, 2000; *Wang et al.*, 2001] and regional haze [e.g., *Chameides et al.*, 1999]. Other studies have suggested that Chinese and eastern Asian emissions will potentially affect the tropospheric chemistry and radiative balance over the Pacific Ocean [e.g., *Hoell et al.*, 1996, 1997; *Elliott et al.*, 1997; *Huebert et al.*, 2003; *Jacob et al.*, 2003] and the surface air quality in North America [*Jacob et al.*, 1999; *Jaffe et al.*, 1999].

[3] Emission estimates in the 1990s showed that there was a rapid rise in emissions of anthropogenic pollutants such as NO_x and SO_2 from the 1980s to the mid 1990s, and a continuing upward trend was projected for the years beyond [e.g., *Akimoto and Narita*, 1994; *Van Aardenne et al.*, 1999; *Streets and Waldhoff*, 2000].

[4] However, there is evidence to suggest that energy use patterns in China began changing quickly in the late 1990s. Recent estimates of emissions [*State Environmental Protection Administration*, 2002; *Streets et al.*, 2003] have shown that between 1995 and 2000 there was a decreasing trend in SO_2 and NO_x emissions due to the restructuring of China's industrial economy, stricter pollution control measures, and an economic slowdown in the late 1990s. However, it is unclear whether this trend of decreasing emissions, which will be good for the environment, will continue and whether a similar trend is occurring uniformly throughout China. It is therefore crucial that concerted efforts be made to document the trend in emissions and to assess the consequent impact of the changing emissions on the environment.

[5] The measurement of ambient concentrations is integral to understanding the relationship between emissions of pollutants and their environmental impact. Atmospheric concentrations are used to benchmark levels of pollution, document trends in concentration, reconcile emission inventories, elucidate atmospheric processes and constrain chemical transport models. Despite their importance, data on ambient concentrations are sparse in nonurban locations in Asia, particularly in the central and eastern regions of China where large quantities of anthropogenic pollutants are emitted.

[6] *Peng et al.* [1997] and *Luo et al.* [2000] analyzed measurements of O_3 obtained at several rural sites in eastern China in 1994–1995 and found high ozone concentrations in the autumn season. More recently, O_3, its precursor gases and aerosols were measured at several rural sites in the Yangtze River Delta region as part of a cooperative effort with the China-MAP research project. *Wang et al.* [2001] reported seasonal variations in O_3, CO, SO_2 and total reactive nitrogen (NO_y*) mixing ratios at Lin'an during 1999–2000 and observed very high concentrations of CO and SO_2. A follow-up study by *Wang et al.* [2002] found that CO emissions from China could have been underestimated in emission inventories and that the burning of biomass/biofuel was a major source of the elevated levels of CO in the autumn-winter period. *Cheung and Wang* [2001] carried out a detailed analysis of ozone pollution episodes at Lin'an and showed that ozone concentrations were high enough to damage crops grown in the region.

[7] With respect to aerosols, *Xu et al.* [2001] presented fine particulate chemical composition and optical measurements made at Lin'an during November 1999 and found very high loadings of particles at the site. Prior studies conducted at Lin'an in February and March 1994 as part of the PEM-West program [*Arimoto et al.*, 1997] showed that the concentrations of non-sea-salt sulfate there were higher than at Hong Kong, Cheju (Korea), or Okinawa (Japan).

[8] In the present study, we present measurements of trace gases and aerosols obtained at Lin'an in spring 2001. The aim is to better characterize emissions and ambient concentrations in the spring season and to assess the relationship between gases and aerosol pollutants. This field program was conducted during the same period as the Asian Pacific Regional Aerosol Characterization Experiment (ACE-Asia) and Transport and Chemical Evolution over the Pacific (TRACE-P) intensive campaigns over the western Pacific region [*Huebert et al.*, 2003; *Jacob et al.*, 2003]. Our measurements shed light on the characteristics of emissions in the inland Asian continental region, which can aid the interpretation of data collected in downwind locations.

[9] In this paper, we first examine the overall concentrations at Lin'an in spring 2001 and compare these observations with previous results for 1999–2000 and with measurements obtained at a South China coastal site in Hong Kong during the same time period. We then examine the interspecies relationships among the measured trace gases and aerosols, and assess the degree of atmospheric processing using relevant chemical ratios. We reexamine the issue of biomass/biofuel burning and compare the measured ratios to emission ratios from the latest emission inventories. We also compare our ground-based results with those obtained on the TRACE-P DC-8 and P-3B aircraft.

2. Experiment

[10] The study was carried out at the Lin'an Baseline Air Pollution Monitoring Station (30°25′N, 119°44′E, 132 m a.s.l., see Figure 1). A detailed description of the surround-

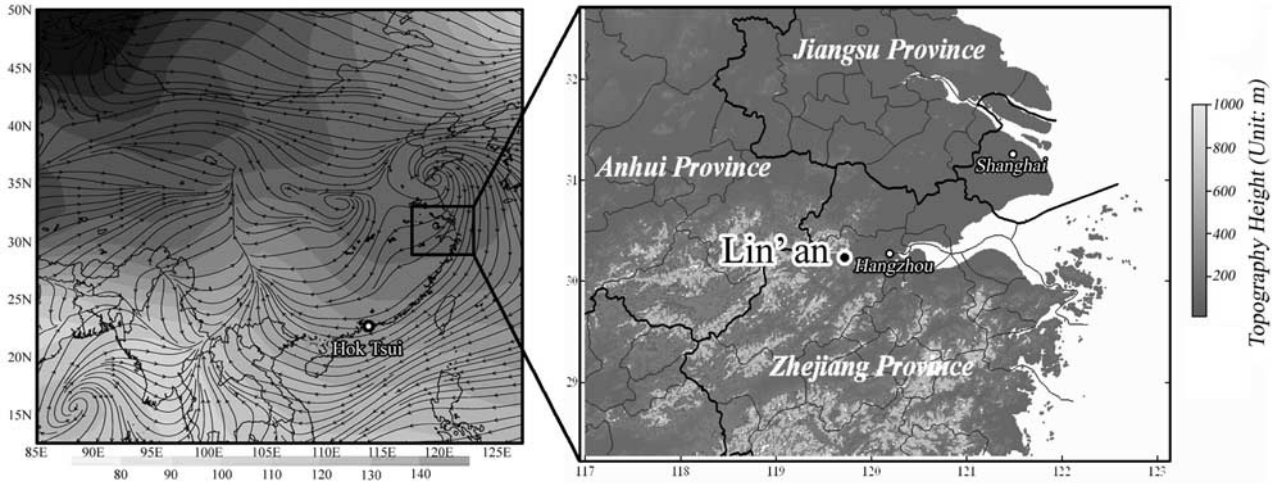

Figure 1. Location of Lin'an in eastern China and mean geopotential height and streamlines for 18 February to 30 April 2001. (The plots were made using NCEP/NCAR reanalysis data available at http://www.cdc.noaa.gov/cdc/data.ncep.renalysis.html.) A South China coastal site (Hok Tsui) in Hong Kong, against whose data the Lin'an data are compared, is also shown.

ings has been given by *Wang et al.* [2001, 2002]. Briefly, the site is located in a hilly agricultural/forested area on the southern edge of the Yangtze River Delta. It is 53 km west and 210 km southwest of the major population centers of Hangzhou and Shanghai, respectively. The township of Lin'an (population ~50,000) is 10 km to the south. Besides these cities, there are a number of smaller pollution sources in rural locations within a 10-km radius from the site, including villages, small industrial plants such as cement kilns and brick kilns, and agriculture-related biomass burning. The land use pattern in the study area is typical of nonurban regions in eastern China.

2.1. Continuous Measurement of Trace Gases

[11] The sampling system and analyzers for measuring O_3, CO, SO_2, NO and NO_y^* employed in the spring 2001 study were identical to those used in our previous measurements at the site [*Wang et al.*, 2002]; thus only a summary is given here. Ambient air was drawn through an 8-m-long PFA Teflon tube (inside diameter = 9.6 mm) connected to a Teflon-made manifold with a bypass pump. O_3 was measured using a UV photometry instrument (Thermo Environmental Instruments (TEI), Inc., model 49). SO_2 was measured by a pulsed UV fluorescence analyzer (TEI, model 43S). CO was detected with a gas filter correlation, nondispersive infrared analyzer (Advanced Pollution Instrumentation, Inc., model 300) with a heated catalytic scrubber for baseline determination. The zeroing for CO was conducted every 2 hours, with each session lasting 12 min.

[12] NO was detected using a chemiluminescence analyzer (TEI, model 42S) with a detection limit of 0.05 ppbv. NO_2 and other reactive nitrogen species were converted to NO on hot molybdenum oxide maintained at 325°C, followed by the quantification of NO using the same chemiluminescence detector. We refer to this measurement as NO_y^* because it does not include aerosol nitrate, which was collected on an inline filter placed upstream from the converter. We also note that some nitric acid may have been absorbed in the sample line (despite the short residence time of <2 s within the sample line). Filter data have shown that the average fraction of nitrate to NO_y (the sum of NO_y^* and NO_3^-) during the study period was about 14%, suggesting that there was a relatively minor contribution of NO_3^- to total reactive nitrogen. The performance of the analyzers was checked on a daily basis by injecting scrubbed ambient air and a calibration standard [*Wang et al.*, 2002]. A data logger was used to control the zero and span tests and to record 1-min data. Hourly averaged values are presented in this paper.

2.2. Methane, NMHCs, Halocarbons, and Alkyl-Nitrates

[13] Two-liter conditioned, evacuated stainless steel canisters each equipped with a bellows valve were filled with whole air samples over a period of about 1 min. The samples were then sent to the University of California at Irvine (UCI) for chemical analysis. Thirty samples were obtained during 2 March to 1 April 2001. One sample was collected at noon each day during the above period. Details of the analytical procedures employed at the UCI laboratory for sample analysis are given by *Colman et al.* [2001] and *Blake et al.* [2003a], and are outlined as follows. For each sample, 1285 ± 2 cm^3 (STP) of air was preconcentrated in a liquid-nitrogen-cooled loop filled with glass beads. After the preconcentration, the trace gas components were revolatilized using a hot water bath then reproducibly split into five streams, with each stream directed to one of five different gas chromatographic column/detector combinations. Electron capture detectors (sensitive to halocarbons and alkyl nitrates), flame ionization detectors (sensitive to hydrocarbons), and quadrupole mass spectrometers (for unambiguous compound identification and selected ion monitoring) were employed. CO was also quantified from the canister samples by first reducing CO to methane, followed by gas chromatographic analyses with a flame ionization detector.

2.3. Fine Aerosol Composition

[14] Eighteen Teflon filter samples and nine Quartz filter samples were collected every other day during 10 March to 9 April 2001. An Andersen PM2.5 RAAS-2.5-1 ambient air

sampler (Thermo Electron Corporation, Waltham, Massachusetts) was employed to collect samples, with a flow rate maintained at 16.7 L min^{-1}. The sample collection time was approximately 24 hours starting at 0900 local time (LT). Chemical analyses of the Teflon filters (2 μm pore size and 47 mm diameter, Pall Gelman, Inc.) were performed for metal elements, water-extractable metals and ions at the Carlsbad Environmental Monitoring and Research Center of New Mexico State University.

[15] One half of each Teflon filter was digested for elemental analyses, and the other half was extracted for analyses of anions, cations, and water-extractable metals. The elemental analyses were conducted by inductively coupled plasma mass spectroscopy (ICP-MS) using a Perkin-Elmer Elan 6000 unit (Perkin-Elmer Corporation, Norwalk, Connecticut), following EPA Method 200.8. Matrix matching was used to prepare calibration standards for the elemental analyses [*Arimoto et al.*, 2002]. The concentrations of ions were determined using a Dionex 500 ion chromatography system (Dionex Corporation, Sunnyvale, California). Nitrate (NO_3^-) and sulfate (SO_4^{2-}) in the aqueous extracts of both sets of filters were separated using an AS-14 column. Cations were separated using a CS-12A column. Only sodium (Na^+), ammonium (NH_4^+), potassium (K^+), magnesium (Mg^{2+}), chloride (Cl^-), NO_3^-, and SO_4^{2-} were frequently detected on the Teflon filter samples.

[16] Quartz fiber filters (47 mm diameter, Pallflex 2500 QAO, Pall Gelman, Inc.) were analyzed for elemental carbon and organic carbon (EC and OC, respectively) at the Southern Center for the Integrated Study of Secondary Air Pollutants (SCISSAP) at Georgia Institute of Technology. EC and OC were determined using the Thermal-Optical Transmittance (TOT) technique, which is based on the thermal-optical transmittance properties of a quartz filter containing carbon residue [*Baumann et al.*, 2003]. The analysis proceeded essentially in two stages. First, OC was volatilized from the sample in a pure helium atmosphere as the temperature was stepped from 340°C to 475°C to 615°C to 870°C within 4.16 min. Evolved carbon was catalytically oxidized to CO_2 in a bed of granular MnO_2 (held at ~900°C), reduced to CH_4 in an Ni/firebrick methanator (~500°C) and quantified as CH_4 using a flame-ionization detector. During the second stage of the analysis, pyrolysis correction and EC measurement were made. The oven temperature was reduced, an oxygen (10%)-helium mix was introduced, and the oven temperature was then raised from 550°C to 625°C to 700°C to 775°C to 850°C to 870°C within another period of 5.25 min. As oxygen entered the oven, pyrolytically generated EC was oxidized and a concurrent increase in filter transmittance occurred. The transmittance was monitored by passing a He/Ne laser light through the filter. The point at which the filter transmittance reached its initial value was defined as the "split" between organic and elemental carbon. Carbon evolved prior to the split was considered "organic," and carbon volatilized after the split was "elemental." The organic carbon concentrations were then multiplied by a factor of 1.4 to account for the mass of hydrogen and oxygen associated with carbon [*White and Roberts*, 1977; *Japar et al.*, 1984]. Therefore the organic carbon in this paper is reported as particulate organic matter (POM) whereas elemental carbon is reported as carbon (C).

2.4. Note on Regression Analysis

[17] Much of the data analysis in this paper involves fitting a straight line to the concentrations of a pair of concurrently measured species. Because the two atmospheric variables under consideration are both subject to measurement errors, we have applied a fitting procedure known as the reduced major axis (RMA) method, as descried by *Hirsch and Gilroy* [1984]. These authors concluded that RMA is more appropriate than the ordinary least square regression as it more accurately reflects the relationships between geophysical variables. RMA has been used by other researchers in analyzing air quality and atmospheric chemistry data [e.g., *Keene et al.*, 1986; *Arimoto et al.*, 1995; *Freijer and Bloemen*, 2000; *Ayers*, 2001]. We have also tested the level of significance for the regression results, using two-tailed *t* tests. Only those regression results with significance levels greater than 95% (i.e., $p < 0.05$) are shown in the plots and used in the discussion.

3. Results and Discussion

3.1. Abundance and Variations of Gases and Aerosols

[18] The meteorological synoptic features over eastern Asia in spring 2001 have been discussed by *Fuelberg et al.* [2003]. Figure 1 presents the mean geopotential height and streamlines at 1000 hPa for 18 February to 30 April 2001 and shows that there was a predominant northeasterly flow in the boundary layer of southern and eastern China. The plots were made using NCEP/NCAR reanalysis data available at http://www.cdc.noaa.gov/cdc/data.necp.reanalysis.html. Surface winds at the Lin'an station were, however, light and variable because of the hilly terrain. Frequent cloudy conditions were also observed during the study period. Analysis of previously collected data has shown that strong pollution events at Lin'an were mainly related to the advection of pollutants from local and subregional emissions under weak synoptic winds [*Cheung and Wang*, 2001].

[19] The statistics of the mixing ratios of the measured constituents are summarized in Table 1. The average mixing ratio was 34 ppbv for ozone, 677 ppbv for CO, 15.9 ppbv for SO_2, and 13.8 for NO_y^* during 18 February to 30 April 2001. Compared to the same period in the previous year, these levels were 12%, 14%, and 16% higher in 2001 for CO, SO_2, and NO_y^*, respectively. In March 2001, when most of the canister and aerosol samples were collected, the monthly mean was comparable for CO (difference = 1%) and NO_y^* (6%), but was higher for SO_2 (by 14%), compared to March 2000. The average diurnal cycles (in local standard time) are shown in Figure 2. They indicate that the mixing ratios of primary pollutants decreased during the daytime, which can be attributed to an enhanced dilution of the convective boundary layer. Similar diurnal profiles were observed for these gases in the previous year [*Wang et al.*, 2002] and for the aerosol scattering and absorption coefficients measured in November 1999 [*Xu et al.*, 2001]. O_3 and the NO/NO_y^* ratio showed a diurnal cycle typically seen in nonurban locations [e.g., *Parrish et al.*, 1993].

Table 1. Statistics of Trace Gases and Aerosols Observed at Lin'an During 18 February to 30 April 2001

	Average	SD	Median	Maximum	Minimum	*N*
Continuously measured trace gases						
O_3, ppbv	34	18	32	95	1	1709
CO, ppbv	677	315	604	2098	183	1708
SO_2, ppbv	15.9	14.6	11.4	82.5	0	1708
NO,[a] ppbv	0.7	1.2	0.3	9.3	0	854
NO_y^*, ppbv	13.8	7.2	12.2	59.5	2.4	1708
Methane and nonmethane NMHCs[b]						
CH_4, ppmv	1.896	0.045	1.888	2.025	1.839	30
Ethane, pptv	3189	717	3084	5565	1978	30
Propane, pptv	1250	526	1149	2580	452	30
i-Butane, pptv	403	296	294	1273	73	30
n-Butane, pptv	453	269	378	1113	99	30
i-Pentane, pptv	345	334	231	1385	53	30
n-Pentane, pptv	140	133	91	489	24	30
Ethene, pptv	1679	1455	1148	5741	317	30
Propene, pptv	298	314	176	1270	41	30
1-Butene, pptv	73	69	51	268	5	30
Ethyne, pptv	2475	1395	2018	6205	705	30
Benzene, pptv	851	730	542	2732	175	30
Toluene, pptv	1529	1608	860	6900	74	30
Ethylbenzene, pptv	200	171	131	643	15	30
m-Xylene, pptv	295	274	260	1112	15	30
p-Xylene, pptv	203	177	189	660	9	30
o-Xylene, pptv	194	159	188	571	12	30
Isoprene, pptv	69	172	22	938	2	30
Halocarbons						
F-11, pptv	288	18	281	345	270	30
F-12, pptv	571	15	568	600	542	30
F-113, pptv	87	8	86	122	81	30
HCFC 22, pptv	180	27	172	254	147	30
CH_3Cl, pptv	1108	653	891	3829	544	30
CH_3Br, pptv	14	7	11	45	9	30
Ethyl chloride, pptv	22	16	16	59	7	30
CCl_4, pptv	111	11	108	147	100	30
C_2Cl_4, pptv	26	21	18	90	7	30
CH_2Cl_2, pptv	83	75	54	419	31	30
$MeCCl_3$, pptv	47	3	47	52	41	30
$CHCl_3$, pptv	52	104	23	576	11	30
1,2-DCE, pptv	82	113	38	487	10	30
Major PM2.5 composition						
OC,[c] $\mu g/m^3$	21.5	7	18.9	33.7	9.5	9
EC, $\mu g/m^3$	2.5	0.7	2.2	3.7	1.8	9
SO_4^{2-}, $\mu g/m^3$	17.3	6.6	16.5	33.6	8.1	18
NO_3^-, $\mu g/m^3$	6.5	4	6.3	15.6	0.5	18
NH_4^+, $\mu g/m^3$	8.7	3.3	9.3	16.2	3.8	18
Na^+, $\mu g/m^3$	0.2	0.1	0.2	0.4	0.1	18
K^+, $\mu g/m^3$	1.7	0.8	1.5	3.5	0.8	18
Mg^{2+}, $\mu g/m^3$	0.3	0.1	0.2	0.5	0.2	12
Cl^-, $\mu g/m^3$	1	0.3	1	1.7	0.5	18

[a]Only data taken between 0600 and 1700 LT were used for the NO statistics here.
[b]NMHCs and halons were determined from whole air samples collected from 2 March to 1 April 2001; aerosol samples were collected during a 24-hour period from 10 March to 9 April 2001.
[c]OC is reported as organic particulate matter, i.e., organic carbon ($\mu gC/m^3$) × 1.4; EC is reported as elemental carbon ($\mu gC/m^3$).

[20] The most abundant NMHC was ethane (mean ± standard deviation = 3189 ± 717 pptv), followed by ethyne (2475 ± 1395 pptv), ethene (1679 ± 1455 pptv), and toluene (1529 ± 1608 pptv). Their mean values were similar to those obtained in autumn 1999 at the site for ethane (3351 ± 921 pptv) and ethyne (2603 ± 880 pptv), and were smaller compared to the 1999 values of ethene (3068 ± 1311 pptv) and toluene (2544 ± 1654 pptv) (N = 16). Methyl chloride (CH_3Cl), which was the dominant halocarbon measured, had a mean value of 1108 (±653) pptv compared to 1350 (±430) pptv in autumn 1999. In general, organic species had lower concentrations in the spring season. For the major components of PM2.5, the mean concentration was 21.5 $\mu g/m^3$ for organic carbon (as POM), 17.3 $\mu g/m^3$ for sulfate, 6.5 $\mu g/m^3$ for nitrate, 8.7 $\mu g/m^3$ for ammonium, and 2.5 μg of C/m^3 for elemental carbon.

[21] During the same time period as studies at Lin'an, trace gases and aerosol elemental compositions were measured at a coastal site (Hok Tsui) in Hong Kong [*Wang et al.*, 2003], which is located approximately 980 km southwest of Lin'an (Figure 1). Since the prevailing winds in the South China coastal region are northeasterly in spring, eastern China could be a source region for the air pollutants measured in Hong Kong. Thus it is of interest to see if the behavior of trace gases measured at the two sites show any relationships. In general, the mixing ratios of the primary pollutants were higher at the eastern China site. For example, the average CO mixing ratio was 677 (±315) ppbv at

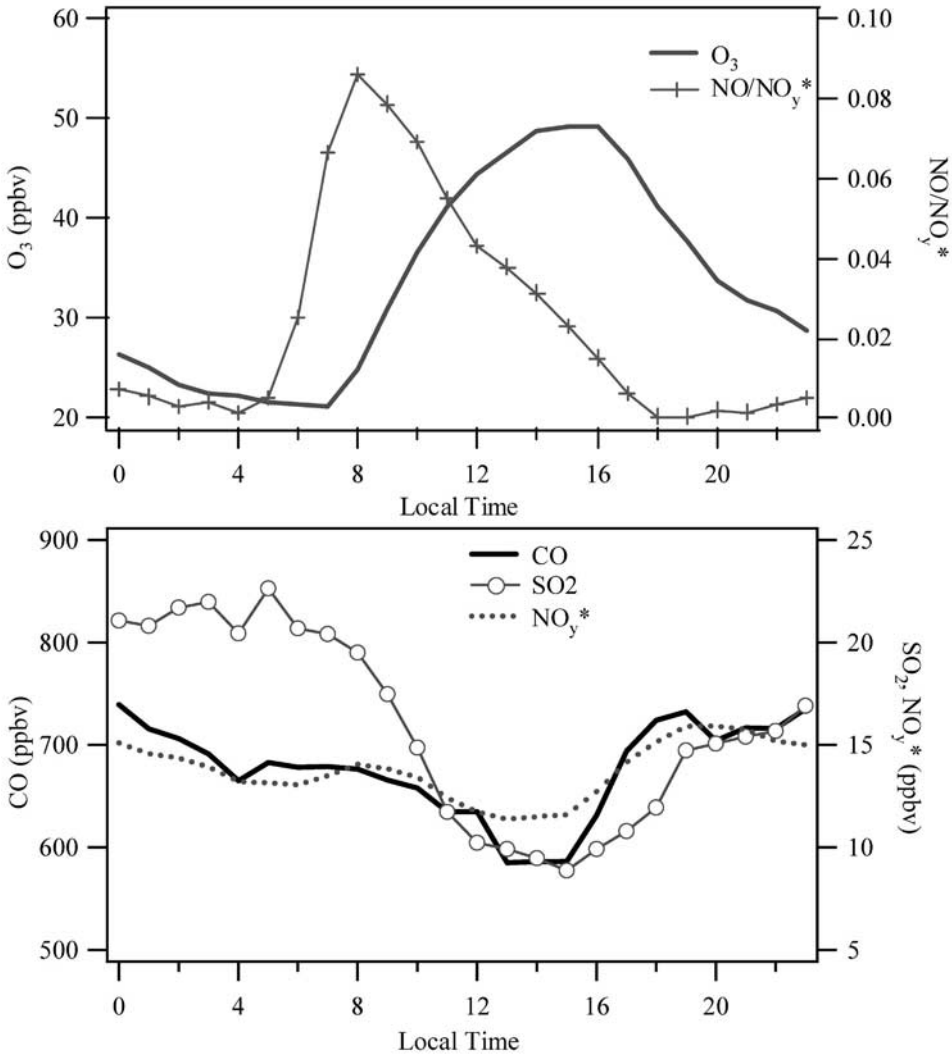

Figure 2. Average diurnal variations of O_3, CO, NO_y^*, SO_2, and NO/NO_y^* at Lin'an during 18 February to 30 April 2001.

Lin'an versus 404 (±228) ppbv at Hok Tsui; SO_2 was substantially higher at Lin'an (15.9 ± 14.6 versus 1.8 ± 3.0 ppbv); and NO_y was 13.8 ± 7.2 ppbv at Lin'an compared to 10.4 ± 10.7 ppbv at Hok Tsui. NMHCs and halons also exhibited higher values at the eastern site. The higher concentrations of these substances at the eastern site are expected because of the stronger anthropogenic emissions in the eastern region compared to those in the southern coastal areas.

[22] The ethyne/CO and propane/ethane ratios, which are measures of atmospheric processing [e.g., *Smyth et al.*, 1999], indicated that the air masses sampled at the Hok Tsui site were more "aged" than the air masses at Lin'an. As a result, higher mixing ratios of O_3 were observed at the southern site (45 ppb ± 19 at Hok Tsui versus 34 ± 18 ppbv at Lin'an). NO was an exception. Its daytime mixing ratio was higher at the southern site: 2.7 ± 8.6 pptv versus 0.7 ± 1.2 ppbv. The abundant NO and a larger NO to NO_y ratio at Hok Tsui resulted from fresh emissions of NO from ships in the coastal waters adjacent to the study site [*Wang et al.*, 2003].

[23] Figure 3 compares daily average mixing ratios of ozone and CO at Lin'an and Hok Tsui. While the magnitude and the short-time variability (i.e., hourly to daily) of O_3 differed between the eastern and southern sites, the synoptic-scale trends were in phase. (Daytime (0800–1959 LT) average O_3 showed a similar synoptic result with a smaller difference in absolute concentration compared to the 24-hour mean.) The above result suggests that large-scale synoptic conditions may have affected the O_3 behavior at both sites. By contrast, no temporal relationship was shown for CO between the two sites, reflecting the influences of emission and meteorology on a subregional scale.

3.2. Relationships Between Trace Gases and Aerosol Composition

3.2.1. Ozone Versus CO, NO_y^*, and SO_2

[24] In the boundary layer of industrialized regions such as eastern China, ozone is expected to originate primarily from photochemical production involving volatile organic compounds and oxides of nitrogen. Stratospheric intrusion is also known to be at maximum strength in spring [e.g.,

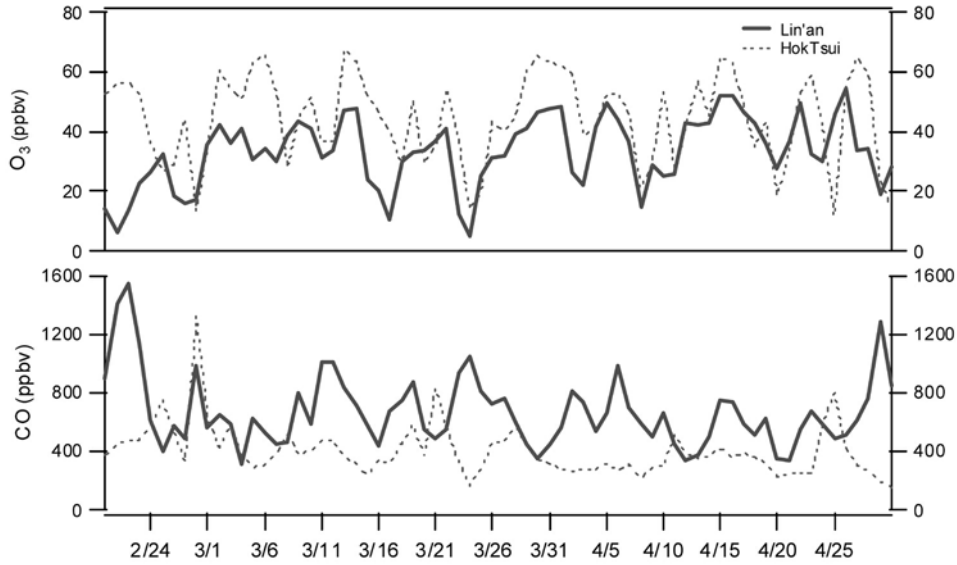

Figure 3. Daily average mixing ratios of ozone and CO measured at Lin'an and Hok Tsui during 18 February to 30 April 2001.

Austin and Midgley, 1994]. Ozonesonde data at Lin'an in spring 2001 showed that the intrusion was most evident in the upper to middle troposphere above Lin'an, but had no obvious influence on surface ozone concentrations [*Chan et al.*, 2003].

[25] CO is produced from the incomplete combustion of fossil fuel and biomass/biofuel; NO_y is generated as NO_x during high-temperature combustion; and SO_2 is mainly produced by burning coals containing sulfur. Positive correlations among O_3, CO, and NO_y are expected in photochemically "aged" air masses [e.g., *Trainer et al.*, 1993; *Parrish et al.*, 1998]. We examined the Lin'an data for relationships among these species. Figure 4 shows scatterplots for O_3 versus CO, NO_y^*, and SO_2 in the afternoon periods (1300–1500 LT) during which photochemical activity tends to reach its peak during a day. Some moderately high ozone events (mean hourly O_3 mixing ratio = 60–90 ppbv) were observed in April, but overall, there is a lack of a correlation between O_3 and CO and NO_y^* (r^2 = 0–0.02). Removing data points with $NO/NO_y^* > 0.01$ (representing fresh emissions) slightly improved the correlations (see Figure 4). In contrast, good correlations between O_3 and CO and NO_y^* were observed in the summer months (June–September) at Lin'an (r^2 = 0.64) [*Wang et al.*, 2001]. The difference in the correlation can be explained by more active photochemistry in summer relative to spring. It is interesting to see that O_3 was better correlated with SO_2 than with CO and NO_y^* (Figure 4), suggesting that some of the O_3 observed in the spring was transported with SO_2.

3.2.2. CO Versus NO_y^* and SO_2

[26] Relationships among CO, NO_y^*, and SO_2 can provide insights into the sources of these compounds in the study region. Scatterplots of CO, NO_y^*, and SO_2 in spring 2001 show that CO and NO_y^* were moderately correlated (r^2 = 0.4), but the SO_2-NO_y^* relationship was more scattered (Figure 5).

[27] To examine the data for temporal trends, the complete data set was stratified by month. A stronger CO-NO_y^* correlation was found in March relative to the full data set. Given that March was the month in which most of the organic samples (29 out of 30) and a majority of the aerosol samples were collected, the data for that month should be most useful in revealing the relationships among the measured species. Figure 6 shows the scatterplots of CO, NO_y^*, and SO_2 in March. The CO-NO_y^* slope was 37 (ppbv/ppbv) with an intercept of 163 and r^2 of 0.59. The slope can be interpreted as the emission ratio provided that CO is not produced in significant amount through oxidation of hydrocarbons and that NO_y is not removed from the atmosphere between emission and sampling. The intercept is the regional background of CO. Similar to the overall data set, SO_2 showed a weak correlation with CO and NO_y^* in March. This was also observed in our previous study [*Wang et al.*, 2002] suggesting that the SO_2 was either emitted from sources different from those for CO and NO_y^* or that these sources have variable emission ratios of SO_2 relative to NO_y^* and CO.

[28] A comparison of the above results with our data obtained in 1999–2000 [*Wang et al.*, 2002] indicates a smaller CO-NO_y^* slope in March 2001 than in September–December 1999. The large CO-NO_y^* slopes in autumn 1999 (50–70 ppbv/ppbv based on RMA and 30–40 ppbv/ppbv by the ordinary linear regression), together with a strong correlation between CO and the biomass-burning tracer CH_3Cl, are interpreted as indications of the burning of agricultural residues after the summer harvest season [*Wang et al.*, 2002]. In section 3.3, we will discuss in more detail how the measured slopes in the present study compare with emission ratios from the emission inventories, and the extent of biomass burning in spring 2001.

3.2.3. CO Versus NMHCs and Halocarbons

[29] As previously mentioned, CO is emitted primarily from the incomplete combustion of fossil fuels and by the burning of vegetation. The CO sources also emit some NMHCs and halocarbons (e.g., ethyne from vehicle exhaust) and sometimes colocate with halocarbon emission

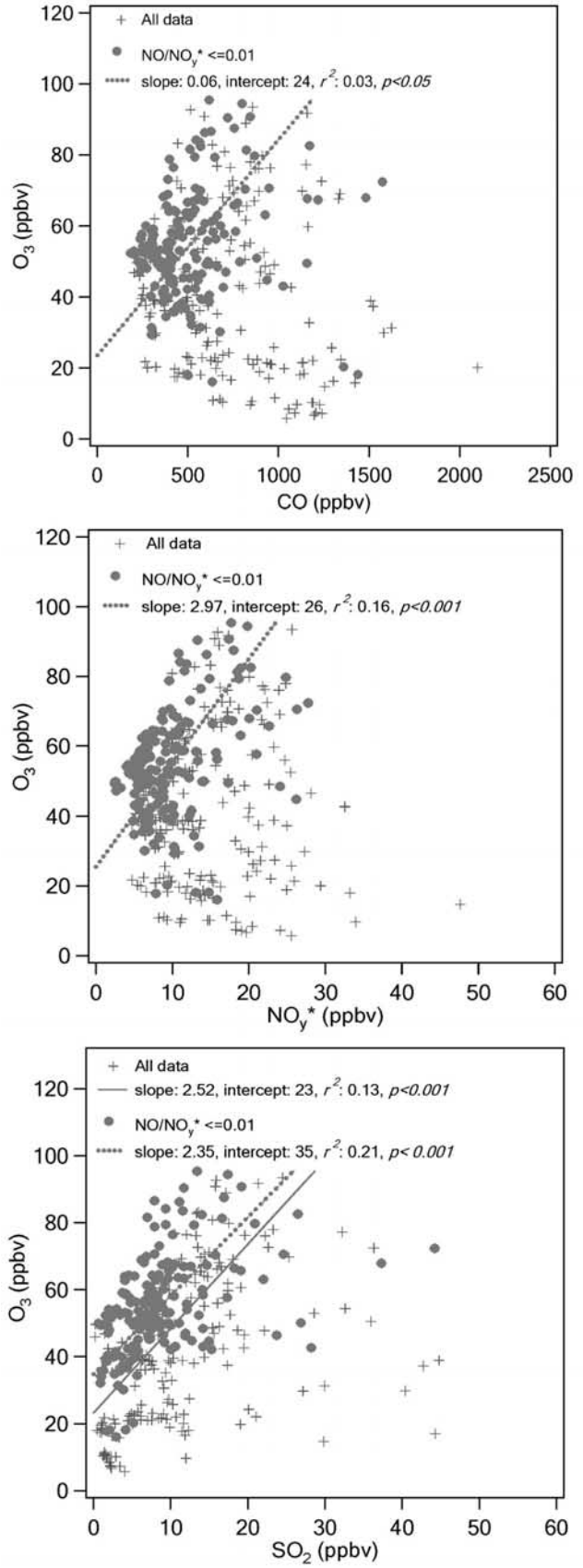

Figure 4. Scatterplots for O_3 versus CO, NO_y^*, and SO_2 for 1300–1500 LT during 18 February to 30 April 2001 at Lin'an. All data and data associated with $NO/NO_y^* \leq 0.01$ are shown.

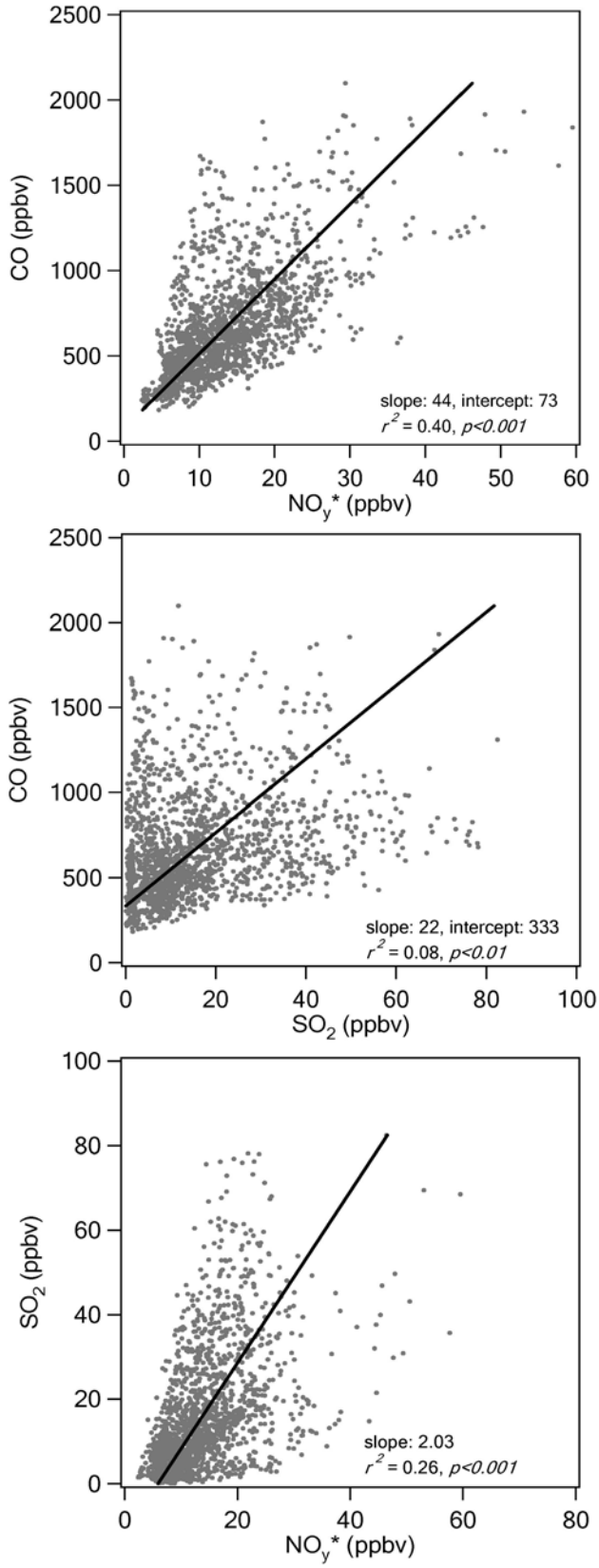

Figure 5. Scatterplots of CO, NO_y^*, and SO_2 during 18 February to 30 April 2001 at Lin'an.

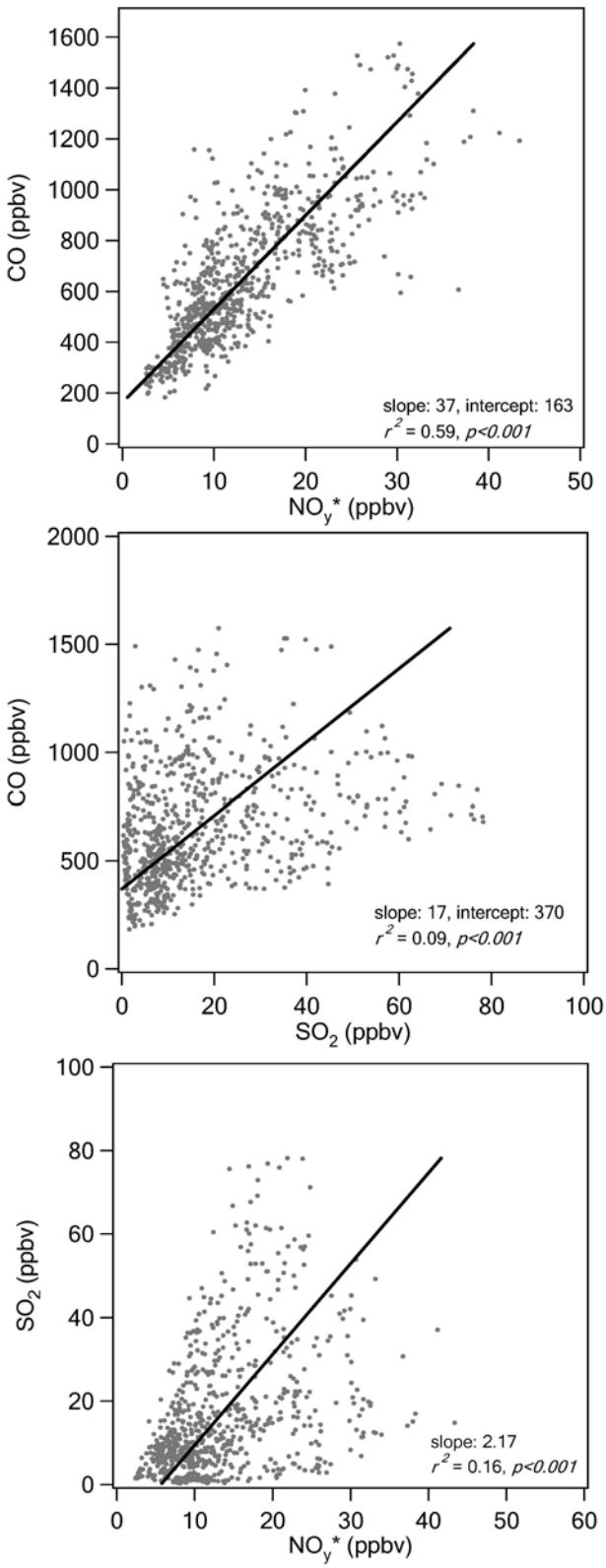

Figure 6. Scatterplots of CO, NO_y*, and SO_2 in March 2001 at Lin'an.

sources. The relationship of CO with NMHCs and halocarbons can thus provide useful information on the emission signatures. Figure 7 shows the scatterplots of CO with selected NMHCs and halocarbons. As expected, CO showed a strong correlation with two combustion-related species: ethyne (C_2H_2, $r^2 = 0.86$) and benzene (C_6H_6, $r^2 = 0.80$). It also correlated well with methane (CH_4, $r^2 = 0.73$), ethane (C_2H_6, $r^2 = 0.78$), propane (C_3H_8, $r^2 = 0.77$), and ethene (C_2H_4, $r^2 = 0.66$). Interestingly, CO showed a moderate correlation with the biomass-burning tracer CH_3Cl ($r^2 = 0.59$), and also with C_2Cl_4 ($r^2 = 0.54$) and F-11 ($r^2 = 0.57$). Tetrachloroethene is primarily released from urban/industrial sources [*Wang et al.*, 1995], as is F-11. This observation contrasts with our previous result in autumn 1999, which showed a strong correlation with CH_3Cl ($r^2 = 0.83$) but a poor correlation with C_2Cl_4 ($r^2 = 0.12$) and F-11 ($r^2 = 0.11$) [*Wang et al.*, 2002]. An examination of the scatterplots of CH_3Cl versus C_2Cl_4 and F-11 revealed that CH_3Cl had a weak correlation with C_2Cl_4 ($r^2 = 0.32$, $p < 0.001$, not shown), but moderate correlation with F-11 ($r^2 = 0.53$, $p < 0.001$, not shown). Could the latter suggest a strong urban/industrial source for CH_3Cl in the study region? We compared a few urban samples collected in the Hangzhou metropolitan area and within the township of Lin'an with samples obtained on the same day at the rural Lin'an site. The results showed comparable CH_3Cl concentrations in the rural and urban areas. For example, in one case, two samples collected in urban Hangzhou showed a CH_3Cl mixing ratio of 1878 pptv (CO = 959 ppbv, from the rooftop of a four-story building) and 2304 pptv (CO = 1221 ppbv, collected adjacent to a road), as compared to a mixing ratio of 2212 pptv collected a few hours before at the Lin'an site (CO = 944 ppbv). In another case, a sample collected in Lin'an township showed a CH_3Cl mixing ratio of 1234 pptv (CO = 731 pptv), as compared to 1539 pptv (CO = 767 ppbv) obtained at the rural site at about same time. These results suggest that rural areas are important source regions for CH_3Cl, reconfirming the hypothesis that CH_3Cl is emitted in significant quantities from the burning of biomass/biofuel in rural locations. Therefore the correlations of CO with CH_3Cl, C_2Cl_4, and F-11 at Lin'an suggest the impact of mixed biomass/biofuel burning and urban/industrial sources in the spring season. Similar correlations have been observed at the South China site in spring 2001 [*Wang et al.*, 2003].

[30] Table 2 presents the slopes of the regressions for selected NMHCs and halocarbons against CO at Lin'an and Hok Tsui in Hong Kong. The two sites had similar $\Delta C_2H_2/\Delta CO$, $\Delta C_6H_6/\Delta CO$ and $\Delta C_2Cl_4/\Delta CO$, while the eastern Lin'an site appeared to have smaller slopes for light alkanes, but a much larger slope of CH_3Cl relative to CO. The large $\Delta CH_3Cl/\Delta CO$ at the eastern site implies that the burning of biomass/biofuel produces significant quantities of CH_3Cl. Table 2 also lists the slopes of some species observed on the TRACE-P DC-8 and P-3B aircraft in air masses originating from source regions such as "South China," "North China" and "Japan + Korea" [*Blake et al.*, 2003b]. The slopes of C_2H_6 and C_3H_8 relative to CO measured at the site in inland eastern China were lower (by a factor of ~2.2–2.5) than those observed on the aircraft for air masses originating from industrialized Japan and South Korea. This can be attributed to strong emissions of CO in China. The site in eastern China also had a much higher (4.7 times) value of $\Delta CH_3Cl/\Delta CO$. By contrast, the C_2H_2-CO slope for the Lin'an site was similar to that in the air mass sampled on the TRACE-P aircraft for "Japan + Korea," suggesting

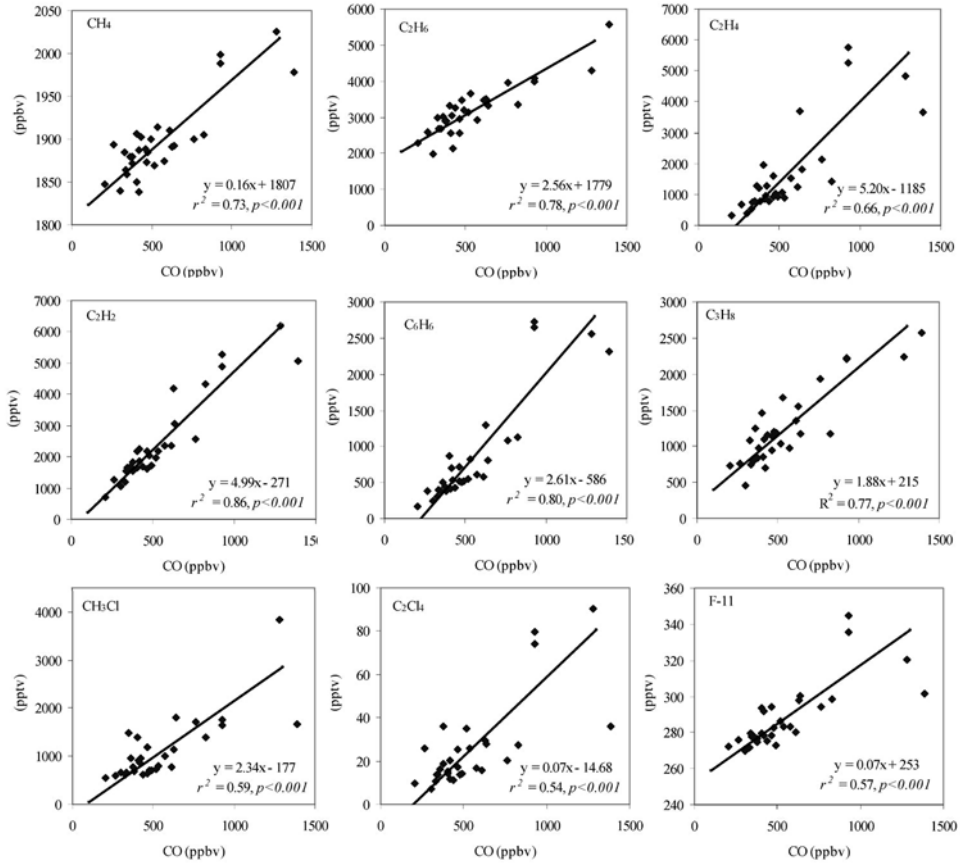

Figure 7. Scatterplots of CO and selected NMHCs and halons collected between 2 March and 1 April 2001 at Lin'an.

that different combustion processes can generate similar $\Delta C_2H_2/\Delta CO$. However, an inconsistent result was found between inland Lin'an and aircraft data for the air mass from "South China" (where Lin'an is located). While the aircraft-observed $\Delta C_2H_2/\Delta CO$ and $\Delta C_3H_8/\Delta CO$ from the "South China" region were very close to those observed at the Lin'an site, the $\Delta C_2H_6/\Delta CO$ was a factor of 1.9 lower at the inland site, while $\Delta CH_3Cl/\Delta CO$ was a factor of 4.2 higher. These results imply that different air masses were sampled at the surface site and on the aircraft.

3.2.4. Interrelationships Among Aerosol Components

[31] As previously mentioned, 18 fine aerosol samples were collected on Teflon filters and analyzed for water-soluble ions and trace metals, while another nine samples were collected on quartz filters and examined for organic and elemental carbons. Correlation plots showed that OC and EC were weakly correlated ($r^2 = 0.34$), suggesting that they were sometimes emitted from different sources. Ammonium was strongly correlated with sulfate ($r^2 = 0.89$) and nitrate ($r^2 = 0.72$), and had a good correlation with potassium ($r^2 = 0.61$). The ambient levels of ammonium ions were sufficiently high to fully neutralize the sulfates and nitrates (see Figure 8), indicating that large amounts of ammonia resulted from the agricultural practices within the region. This observation contrasts with that of an incomplete neutralization of sulfates and nitrates by ammonia (NH_3) in urban Beijing and Shanghai [*Yao et al.*, 2002]. At Lin'an, fine nitrates were strongly correlated with sulfate ($r^2 = 0.70$). The large nitrate/sulfate ratios (mean mass ratio = 0.42) suggests that the reaction $NH_3(g) + HNO_3(g) \rightarrow NH_4NO_3(s)$ favored the presence of solid-phase ammonium nitrates, probably because of the

Table 2. Slopes of Selected NMHCs and Halons to CO at Lin'an and Hok Tsui (Hong Kong) and From TRACE-P Aircraft in Spring 2001[a]

	$\Delta C_2H_6/\Delta CO$	$\Delta C_2H_2/\Delta CO$	$\Delta C_3H_8/\Delta CO$	$\Delta C_6H_6/\Delta CO$	$\Delta CH_3Cl/\Delta CO$	$\Delta C_2Cl_4/\Delta CO$
Linan	2.6 ± 0.46	5.0 ± 0.72	1.9 ± 0.35	2.6 ± 0.45	2.3 ± 0.58	0.07 ± 0.02
Hok Tsui[b]	4.8 ± 1.19	5.5 ± 0.57	2.9 ± 0.74	2.3 ± 0.46	1.1 ± 0.33	0.08 ± 0.02
TRACE-P[c]						
"South China"	4.9	4.7	1.8	–	0.54	–
"North China"	3.4	3.8	1.1	–	0.34	–
"Japan + Korea"	6.5	4.7	4.2	–	0.50	–

[a]Uncertainties are given as 95% confidence intervals.
[b]*Wang et al.* [2003].
[c]*Blake et al.* [2003b].

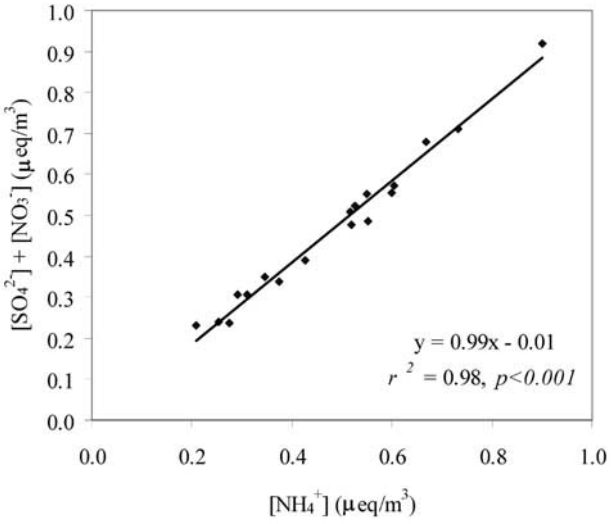

Figure 8. Scatterplot of ammonium versus the sum of nitrate and sulfate.

abundant NH_3 in the study region. Silicon (Si) in fine aerosols was not well correlated with soil tracers such as aluminum (Al) (r^2 = 0.22), iron (Fe) (r^2 = 0.28), and manganese (Mn) (r^2 = 0.13), but was highly correlated with calcium (Ca) (r^2 = 0.75) and chromium (Cr) (r^2 = 0.83). These results suggest the presence of sources for fine Si and Ca other than soils. Fugitive emissions from cement plants in the study region are a possible source given that Si and Ca are two major chemical components in cement.

3.2.5. Relationships Between Gases and Aerosols

[32] The concurrent measurements of gases and aerosols in spring 2001 present an opportunity for investigating their relationships. As shown in Figure 9, the time-matched (24-hour average) CO mixing ratio had a good positive correlation with organic carbon (r^2 = 0.65, $p < 0.01$) and a moderate correlation with water-soluble potassium (r^2 = 0.53, $p < 0.001$), but no correlation with EC (r^2 = 0.04). SO_2 was correlated with EC (r^2 = 0.56, $p < 0.05$) but not OC (r^2 = 0.17), while NO_y^* showed a weak correlation with OC (r^2 = 0.47, $p < 0.05$).

[33] Water-soluble K^+ is a known tracer of vegetation burning [*Andreae*, 1983]. OC is also emitted in large quantities during the smoldering stage of vegetation burning, whereas EC is primarily emitted in the flaming stage [*Kaufman et al.*, 2002]. Coal burning is another major source for EC, and OC is also emitted during the burning of liquid fuels such as gasoline and kerosene [e.g., *Streets et al.*, 2003]. The correlations between CO, OC, and K^+ suggest that biomass/biofuel burning (mostly smoldering) in the study area is an important source of these species. On the other hand, the correlation between SO_2 and EC implies a contribution from coal burning for these two compounds. A good correlation of NO_y with CO and OC and a lack of correlation with SO_2 suggests that NO_y is probably also mainly emitted from biomass/biofuel burning.

[34] CO also showed moderate to good correlations with secondary aerosol ions such as NH_4^+ (r^2 = 0.62, $p < 0.001$) and SO_4^{2-} (r^2 = 0.58, $p < 0.001$), but SO_2 and NO_y^* did not show such relationships. This may suggest that ammonium sulfate and some of the CO were transported to the study site.

3.2.6. Indicators of Atmospheric Processing

[35] Ambient concentrations can be used to evaluate the extent of photochemical processing and dynamic mixing. This can be done by examining the ratio of a pair of species with different chemical lifetimes, such as C_2H_2/CO and C_3H_8/C_2H_6 [e.g., *Smyth et al.*, 1999], or the ratio of a secondary pollutant to the sum of all secondary pollutants and their parent primary pollutant, such as $[SO_4^{2-}]/([SO_2] + [SO_4^{2-}])$ and $[NO_3^-]/([NO_y^*] + [NO_3^-])$.

[36] The average (±standard deviation) $[SO_4^{2-}]/([SO_2] + [SO_4^{2-}])$ molar ratio at Lin'an in spring 2001 was 0.24 (±0.10), while $[NO_3^-]/([NO_y^*] + [NO_3^-])$ was 0.14 (±0.06). *Ma et al.* [2003] found $[SO_4^{2-}]/([SO_2] + [SO_4^{2-}])$ ratios of 0.42, 0.51 and 0.89 in three plumes sampled on the TRACE-P P-3B aircraft over the western Pacific rim. The relatively small fraction of sulfate and nitrates at Lin'an compared to those observed on the aircraft indicates that boundary layer air masses at Lin'an were quite fresh with respect to photochemical processing. The small faction of nitrate also implies that our NO_y^* measurement (which did not include nitrate particles) was a good representation of total reactive nitrogen (NO_y).

[37] The relatively fresh air masses at Lin'an were also indicated by large ratios of C_2H_2/CO (4.4 ± 0.8, pptv/ppbv) and C_3H_8/C_2H_6 (0.38 ± 0.08 pptv/pptv). For comparison, *Russo et al.* [2003] reported mean C_2H_2/CO ratios of 3.9 (±1.3) and 2.5 (±1.2) in the "Central" and "Coastal" source regions of China, and average C_3H_8/C_2H_6 ratios of 0.35 (±0.09) and 0.19 (±0.12) in these regions, respectively. Our surface measurements at the South China coastal site showed a mean ratio of 3.9 (±0.6) for C_2H_2/CO and 0.33 (±0.08) for C_3H_8/C_2H_6 [*Wang et al.*, 2003].

[38] Because C_2H_2/CO and C_3H_8/C_2H_6 can serve as measures of atmospheric processing, it is of interest to know how gas concentrations vary with these ratios. One would expect to see higher trace gas concentrations as the values of these ratios increase (representing fresher air masses). As shown in Figure 10, CO, NO_y^*, and SO_2 had no relationships with C_2H_2/CO (r^2 = 0.00–0.05). On the other hand, both CO and NO_y^* showed moderate to good positive correlations with C_3H_8/C_2H_6, while SO_2 did not. Scatterplots of individual NMHCs also showed strong correlations with C_3H_8/C_2H_6, but not with C_2H_2/CO, as illustrated for *n*-butane in Figure 10. These results suggest that C_3H_8/C_2H_6 is a better measure of atmospheric processing than C_2H_2/CO for most of the trace gases measured in our study.

3.3. On the Contribution of Biofuel/Biomass Burning at Lin'an and Implications for the Refinement of Emission Inventories

[39] Previous measurements at Lin'an have shown impacts from biomass burning in autumn and there are indications that total emissions of CO from eastern China have been underestimated. The results are briefly summarized here. On the basis of the data collected in 1999–2000, we found that the measured CO-NO_y^* slope derived from the winter and nighttime data set was 36 ppbv/ppbv (determined with ordinary linear regression) [*Wang et al.*, 2002]. (The CO-NO_y^* slope is 46 ppbv/ppbv based on RMA with an

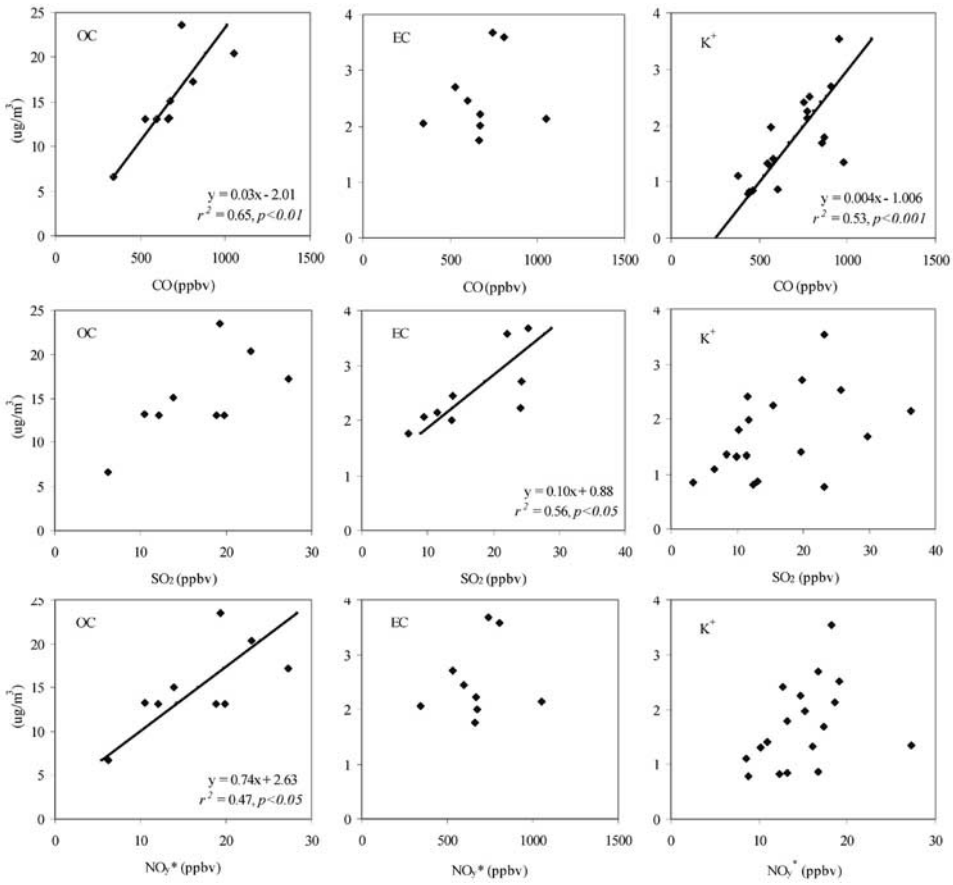

Figure 9. Scatterplots of CO, SO_2, and NO_y^* and time-matched OC, EC, and K^+ during spring 2001. (OC is reported as particulate organic matter, and EC is reported as carbon; see text.)

uncertainty of 0.8 given as the 95% confidence interval.) This was more than 3 times the emission ratio derived from an earlier version of the emission inventories of *Streets et al.* [2003] for the year 2000. The previous inventory did not include open biomass burning. We also found that the CO-NO_y^* slope peaked in September–December 1999 and in June 2000, coinciding with the periods of active open burning of agricultural residues, after the harvesting of summer rice in

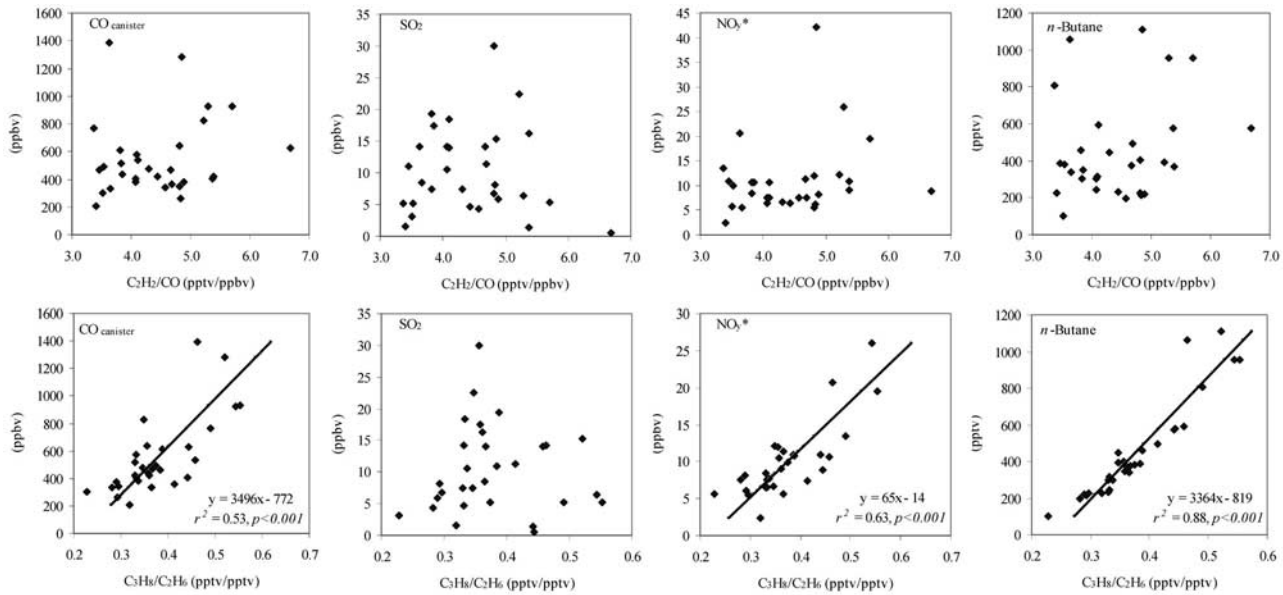

Figure 10. Scatterplots of CO, SO_2, NO_y^*, and *n*-butane with C_2H_2/CO and C_3H_8/C_2H_6. C_2H_2, ethyne; C_3H_8, propane; C_2H_6, ethane.

Table 3. Comparison of Emission Ratios and the Observed Ratios for CO, NO_y^*, and SO_2 at Lin'an in March 2001[a]

	SO_2/NO_y^*	$\Delta CO/\Delta NO_y^*$
Zhejiang	0.88	13
Shanghai	0.97	9
Jiangsu	1.24	14
Jiangxi	1.54	25
Fujian	0.83	22
Anhui	0.92	19
Region average	1.08	16
Measurement inferred	1.29 ± 0.07[b]	37 ± 2

[a]Uncertainties are given as 95% confidence intervals.
[b]Measured value is the average concentration ratio for SO_2/NO_y^* and the regression slope for CO/NO_y^*.

autumn and winter wheat in summer within the study region. In autumn 1999 we also observed strong correlations of CO with the biomass-burning tracer CH_3Cl, and a lack of a correlation with the urban/industrial tracers C_2Cl_4 and F-11. We interpreted these observations as indications of crop residue/biofuel burning, and suggested that biomass/biofuel burning could be a major source of the observed CO and possibly of other trace gases as well. An additional indication of biomass burning was suggested from aerosol measurements at the site in November 1999, which showed a large fraction (~80%) of water-insoluble OC in total OC [*Xu et al.*, 2001]. A study by *Kotchenruther and Hobbs* [1998] found that organic aerosols from biomass burning in Brazil were water insoluble.

[40] It is of great interest to reexamine the issue of biomass burning for the spring season and to compare the springtime ambient trace gas ratios to those from the latest version of emission inventories developed by *Streets et al.* [2003]. Given that early spring is not a harvesting season, one would expect to see less active open burning of agricultural residues than in autumn. Visual observations during our site visits did indeed indicate less intensive burning in spring 2001, compared with the October–November period in 1999.

[41] Data from the canister samples also revealed a smaller biomass-burning signal in spring 2001 than in fall 1999. For example, the NMHC data obtained from 2 March to 1 April 2001 showed a weaker correlation of CO with CH_3Cl and an improved correlation with the industrial tracer of C_2Cl_4 when compared to the samples from 26 October to 2 November 1999. The average CO mixing ratio determined from the canister samples was 551 ± 280 ppbv in spring 2001; this was lower than the average from the autumn 1999 samples (686 ± 204 ppbv). The lower CO levels and a reduced CO-NO_y^* slope in spring 2001 suggested that there is a smaller impact from the burning of vegetation in spring, which can be attributed to the less active burning of crop residues during this season.

[42] How do the ratios observed at Lin'an in spring 2001 compare to the respective ratios derived from the emission inventory of *Streets et al.* [2003] developed for the TRACE-P project for the year 2000? Table 3 shows a comparison of inventory-derived SO_2/NO_y and CO/NO_y ratios for the five provinces surrounding Lin'an and the municipality of Shanghai, as well as the regional average, and the measured SO_2/NO_y^* ratio and CO-NO_y^* slope ($\Delta CO/\Delta NO_y^*$). The measured values are based on the data for March 2001.

[43] The observed mean SO_2/NO_y^* ratio was 1.29 with an uncertainty of 0.07 at 95% confidence level (all ratios expressed as ppbv/ppbv). This ratio agrees well (within 20%) with the inventory value of 1.08 for the region. This is not too surprising, because the inventory is known to compare well with calculations of emissions of SO_2 and NO_x in China by other researchers (see discussion given by *Streets et al.* [2003]), and because emissions in March are believed to be similar to the annual mean according to the seasonality analysis given by *Streets et al.* [2003]. In contrast, the observed $\Delta CO/\Delta NO_y^*$ value (37 ± 2) is more than twice the inventory value (15.6) for the region. Both SO_2/NO_y^* and $\Delta CO/\Delta NO_y^*$ are closer to the ratios for the essentially rural province of Jiangxi (1.54 and 25, respectively) than to the urban ratios of Shanghai (0.97 and 9.2). This is perhaps consistent with the location and surroundings of Lin'an.

[44] These ratio results are in accord with our previous comparison of winter 1999 data with the earlier inventory, which found a comparable observed and inventory-suggested SO_2/NO_y ratio (1.37 versus 1.12), but a much larger observed CO-NO_y slope (44 versus 11). While it is possible that some NO_y components (i.e., nitric acid and aerosol nitrate) could have been removed from air masses because of dry and wet deposition before being sampled, thus making our measured CO-NO_y^* slope larger than the original emission ratio, the good linear correlation between CO and NO_y^* (Figure 6) and the relatively "young" air masses (Figure 10) at Lin'an in March strongly suggest that the larger observed CO-NO_y^* slope was mainly due to an underestimation of CO emissions in the inventory for the study region. We have also found additional evidence for the underestimation of CO by comparing observed NMHC-CO slopes with emission ratios from the inventory (see Table 4). The results show that the observed slopes for ethane, propane, *i*- and *n*-butane, ethene, and ethyne are all smaller than the respective emission ratios relative to CO derived from the inventories. This is consistent with the comparison of CO/NO_y slopes, suggesting that CO emissions have been underestimated in the inventories. In particular, the observed slopes of CO-NO_y^*, propane-CO, butane (sum of *i*- and *n*-butane)-CO, and ethyne-CO suggest that the respective emission ratios would approach the observed values if total CO emissions increased by ~100% for Zhejiang Province.

[45] Underrepresentation of China's CO emissions has also been found by comparing TRACE-P airborne measurements made over the Yellow Sea with modeled CO concentrations [*Carmichael et al.*, 2003; *Palmer et al.*, 2003] and from a recent global CO inverse modeling study by *Kasibhatla et al.* [2002]. With the aid of a back-trajectory analysis, *Carmichael et al.* [2003] attributed the underprediction of CO (and of related species such as SO_2 and BC) in their model to an underestimation of emissions from the domestic use of coal in the central regions of China between Chongqing and Shanghai.

[46] What might be the source of the additional CO observed at Lin'an (and during the TRACE-P flights)? This question is not easy to answer on the basis of the results of our present study. With regard to the inventory, we have conducted several exercises to estimate emission ratios of trace gases by manipulating the inventory of *Streets et al.*

Table 4. Comparison of Observed NMHC/CO Slopes With Ratios From the Inventories for Different Source Categories for Zhejiang Province[a]

	ΔEthane/ΔCO	ΔPropane/ΔCO	ΔButanes/ΔCO	ΔPentanes/ΔCO	ΔEthene/ΔCO	ΔPropene/ΔCO	ΔEthyne/ΔCO	ΔBenzene/ΔCO
BioB	10.7	3.9	0.4	0.1	16.5	7.9	4.6	0.6
Anthro	7.7	4	4.2	2.8	16.9	4.5	9.7	2.4
BioB + Anthro	8	4	3.8	2.5	16.9	4.8	9.3	2.3
Measurement inferred at Lin'an								
Slope	2.6 ± 0.46	1.9 ± 0.35	2.0 ± 0.33	1.7 ± 0.33	5.2 ± 1.17	1.1 ± 0.28	5.0 ± 0.72	2.6 ± 0.45

[a]BioB, biomass burning; Anthro, anthropogenic. Uncertainties are given as 95% confidence intervals.

[2003]. These exercises include (1) an assumption that 100% of crop residues are burned in two months of the year rather than the inventory value of 17%, (2) a sensitivity analysis of the quantities of biofuel likely to be burned in Zhejiang Province, (3) use of larger emission factors for stoves and small industrial plants such as ovens and kilns, and (4) use of a larger emission factor for transportation. It was concluded that within the range of literature-reported emission factors and on the basis of the current best estimate of activity data (see discussion given by *Streets et al.* [2003]), we were unable to identity the missing CO source(s) from the inventory point of view. A systematic survey/test of emission sources (strength and emission ratios) within the study region and in other regions in China will be required to justify more drastic changes of emission ratios and activity data adopted in the current inventories. Such investigations should be carried out in the near future.

[47] *Carmichael et al.* [2003] suggest that an underestimation of residential coal burning could be the cause of elevated CO, BC and SO_2 observations during TRACE-P. It is quite possible that recent estimates of residential coal combustion in China are underreported in national statistics (see discussion given by *Streets et al.* [2003]). However, coal is not a favored residential fuel in the Yangtze delta. Ambient measurements at Lin'an show that CO had no correlation with the coal burning tracer SO_2 (see Figure 5), which strongly suggests that the majority of CO was not from coal burning within the study region.

[48] What else could cause high concentrations of CO at Lin'an in March? It is known that in Southeast Asia and more remote provinces of China such as Yunnan and Guizhou, March is one of the most significant months for biomass burning associated with ''slash-and-burn'' agriculture, where land with trees and shrubs is burned prior to planting in the springtime and land is rotated year-by-year. Emissions of CO are very high at this time of year. Is it possible that this is the cause of regional buildup of CO in south-central China? The air mass dynamics do not seem to support this hypothesis. Most of the high-CO events observed at Lin'an were associated with light synoptic winds, suggesting an origin of adjacent or subregional sources. Also, sounding data at Lin'an in springtime showed that there was little exchange of air masses between the boundary layer and the free troposphere. In addition, observations showed higher average concentrations of CO at night when a nocturnal stable layer was expected to form, preventing downward transport of air masses. All these indications suggest that the CO was not coming from distant sources.

[49] We have also considered the possibility that the Lin'an measurements may be incompatible with the regional inventory, as the trace gases measured at Lin'an are strongly influenced by sources in rural areas with high CO/NO_y ratios (such as biofuel and biomass burning) while the regional inventory also includes large urban sources which are expected to have lower CO/NO_y ratios, as in the case of Shanghai (see Table 4). However, as shown by *Wang et al.* [2002], an examination of the emission ratios in the inventories for rural regions west of Lin'an also indicated a CO/NO_y ratio about 2–3 times lower than the observed slope at Lin'an. This result confirms that CO emission has been underestimated for rural areas surrounding the study site, and possibly for other rural regions as well. Additional comparisons of regional models with a fine-grid resolution with the measurements at Lin'an will be needed to better understand the missing CO source(s) at Lin'an. It is also essential to survey emission sources in study region and to perform measurements in close proximity to emissions—whether from stacks, home chimneys, vehicle tailpipes or fields.

4. Conclusions

[50] We measured trace gases and aerosols at a rural site, Lin'an, in the central-eastern part of China during 18 February to 30 April 2001. Overall, trace gas and aerosol levels at this nonurban site were highly elevated, particularly for CO (mean = 677 ppbv), SO_2 (15.9 ppbv), particulate organic matter (21.5 $\mu g/m^3$) and fine-particle sulfate (17.3 $\mu g/m^3$). Given that the land use pattern surrounding the site is typical of rural regions in eastern China, the results from this study imply widespread regional pollution.

[51] The concurrent measurement of many species yielded important insights about interspecies relationships and emission characteristics in the inland region during the spring season. The results revealed that the sources of pollutants were complex and included the burning of fossil fuels and biomass/biofuels, urban/industrial emissions, and agricultural activities. The biomass-burning signal was not as strong in spring 2001 compared to previous observations in autumn 1999 [*Wang et al.*, 2002]. Fine sulfate and nitrates were fully neutralized by ammonia, suggesting that a large amount of ammonia resulted from agricultural practices in the region. The measurements also revealed relatively ''young'' air masses at the study site, which could undergo photochemical processing as the air masses were transported to regions downwind. The propane to ethane ratio was found to be a better indicator of atmospheric processing, as compared to the ethyne to CO ratio.

[52] Our measurements from eastern China, where large anthropogenic emissions occur, proved to be valuable in validating ''bottom-up'' emission inventories. Through a comparison of observed versus measured slopes/ratios, CO

emissions in the study region were found to have been underrepresented in the current emission inventory. This finding is in accord with our analysis of autumn-winter data previously obtained from this site [*Wang et al.*, 2002]. Additional studies, including a detailed survey of emission sources in the study region and a comparison of ambient data with fine-grid resolution regional models, are required to identify the missing CO source(s) and to investigate its (their) geographical extent.

[53] In view of the complex mixture of chemical signals from different emission sources in nonurban regions of eastern China, studies that combine field measurements with chemical transport models will be needed to elucidate the chemical and transport processes affecting the variations and budgets of trace gases and aerosols. In this connection, our measurements provide an important data set for comparison with modeled results for the central-eastern region of China.

[54] **Acknowledgments.** We thank C. N. Poon, G. P. Liu, L. Y. Chan, C. Y. Chan, and S. C. Zou for their help in deploying our instruments to the study site and Joey Kwok for his assistance in data processing. This study was funded by the Hong Kong Polytechnic University and by the Research Grants Council of the Hong Kong Special Administrative Region (project PolyU 5063/01E to T.W.). R.A. acknowledges support for his effort by a grant from the National Science Foundation of the United States (NSF ATM0002054).

References

Akimoto, H., and H. Narita (1994), Distribution of SO_2, NO_x and CO_2 emissions from fuel combustion and industrial activities in Asia with $1^\circ \times 1^\circ$ resolution, *Atmos. Environ.*, *28*, 213–225.

Andreae, M. O. (1983), Soot carbon and excess fine potassium: Long-range transport of combustion-derived aerosols, *Science*, *220*, 1148–1151.

Arimoto, R., R. A. Duce, B. J. Ray, W. G. Ellis Jr., J. D. Cullen, and J. T. Merrill (1995), Trace elements in the atmosphere over the North Atlantic, *J. Geophys. Res.*, *100*, 1199–1213.

Arimoto, R., R. A. Duce, J. M. Prospero, D. L. Savoie, R. W. Talbot, J. E. Dibb, B. G. Heikes, B. J. Ray, N. F. Lewis, and U. Tomza (1997), Comparisons of trace constituents from ground stations and the DC-8 aircraft during PEM-West B, *J. Geophys. Res.*, *102*, 28,539–28,550.

Arimoto, R., W. Balssam, and C. Schloesslin (2002), Visible spectroscopy of aerosol particles collected on filters: Iron-oxide minerals, *Atmos. Environ.*, *36*, 89–96.

Austin, J. F., and R. P. Midgley (1994), The climatology of the jet stream and stratospheric intrusions of ozone over Japan, *Atmos. Environ.*, *28*, 39–52.

Ayers, G. P. (2001), Comment on regression analysis of air quality data, *Atmos. Environ.*, *35*, 2423–2425.

Baumann, K., F. Ift, J. Z. Zhao, and W. L. Chameides (2003), Discrete measurements of reactive gases and fine particle mass and composition during the 1999 Atlanta Supersite Experiment, *J. Geophys. Res.*, *108*(D7), 8416, doi:10.1029/2001JD001210.

Blake, N. J., D. R. Blake, A. L. Swanson, E. Atlas, F. Flocke, and F. S. Rowland (2003a), Latitudinal, vertical and seasonal variations in C_1-C_4 alkyl nitrates in the troposphere over the Pacific Ocean during PEM-Tropics A and B: Oceanic and continental sources, *J. Geophys. Res.*, *108*(D2), 8242, doi:10.1029/2001JD001444.

Blake, N. J., et al. (2003b), NMHCs and halocarbons in Asian outflow during TRACE-P: Comparison to PEM-West B, *J. Geophys. Res.*, *108*(D20), 8806, doi:10.1029/2002JD003367.

Carmichael, G. R., et al. (2003), Evaluating regional emission estimates using the TRACE-P observations, *J. Geophys. Res.*, *108*(D21), 8810, doi:10.1029/2002JD003116.

Chameides, W. L., et al. (1999), Case study of the effects of atmospheric aerosols and regional haze on agriculture: An opportunity to enhance crop yields in China through emission controls?, *Proc. Natl. Acad. Sci. U. S. A.*, *96*, 13,626–13,633.

Chan, C. Y., L. Y. Chan, H. Cui, X. D. Zheng, Y. Qin, and Y. S. Li (2003), Origin of the springtime tropospheric ozone maximum over east China at Lin'an in year 2001, *Tellus, Ser. B*, *55*, 982–992.

Cheung, V. T. F., and T. Wang (2001), Observational study of ozone pollution at a rural site in the Yangtze Delta of China, *Atmos. Environ.*, *35*, 4947–4958.

Colman, J. J., A. L. Swanson, S. Meinardi, B. C. Sive, D. R. Blake, and F. S. Rowland (2001), Description of the analysis of a wide range of volatile organic compounds in whole air samples collected during PEM-Tropics A and B, *Anal. Chem.*, *73*(15), 3723–3731.

Elliott, S., D. R. Blake, R. A. Ruce, C. A. Lai, I. McCreary, L. A. McNair, F. S. Rowland, and A. G. Russell (1997), Motorization of China implies changes in Pacific air chemistry and primary production, *Geophys. Res. Lett.*, *24*, 2671–2674.

Freijer, J. I., and H. J. Th. Bloemen (2000), Modeling relationships between indoor and outdoor air quality, *J. Air Waste Manage. Assoc.*, *50*, 292–300.

Fuelberg, H. E., C. M. Kiley, J. R. Hannan, D. J. Westberg, M. A. Avery, and R. E. Newell (2003), Atmospheric transport during the Transport and Chemical Evolution over the Pacific (TRACE-P) experiment, *J. Geophys. Res.*, *108*(D20), 8782, doi:10.1029/2002JD003092.

Hirsch, R. M., and E. J. Gilroy (1984), Methods of fitting a straight line to data: Examples in water resources, *Water Resour. Bull.*, *20*(5), 705–711.

Hoell, J. M., D. D. Davis, S. C. Liu, R. Newell, M. Shipham, H. Akimoto, R. J. McNeal, R. J. Bendura, and J. W. Drewry (1996), The Pacific Exploratory Mission-West A (PEM-West A): September–October, 1991, *J. Geophys. Res.*, *101*, 1641–1653.

Hoell, J. M., D. D. Davis, S. C. Liu, R. E. Newell, H. Akimoto, R. J. McNeal, and R. J. Bendura (1997), The Pacific Exploratory Mission West Phase B: February–March, 1994, *J. Geophys. Res.*, *102*, 28,223–28,239.

Huebert, B., T. Bates, P. Russell, J. Seinfeld, M. Wang, M. Uematsu, and Y. J. Kim (2003), An overview of ACE-Asia: Strategies for quantifying the relationships between Asian aerosols and their climatic impacts, *J. Geophys. Res.*, *108*(D23), 8633, doi:10.1029/2003JD003550.

Jacob, D. J., J. A. Logan, and P. P. Murti (1999), Effects of rising Asian emissions on surface ozone in the United States, *Geophys. Res. Lett.*, *26*, 2175–2178.

Jacob, D. J., J. H. Crawford, M. M. Kleb, V. E. Connors, R. J. Bendura, J. L. Raper, G. W. Sachse, J. C. Gille, L. Emmons, and C. L. Heald (2003), The Transport and Chemical Evolution over the Pacific (TRACE-P) mission: Design, execution, and overview of results, *J. Geophys. Res.*, *108*(D20), 9000, doi:10.1029/2002JD003276.

Jaffe, D. A., et al. (1999), Transport of Asian air pollution to North America, *Geophys. Res. Lett.*, *26*, 711–714.

Japar, S. M., A. C. Szkarlat, R. A. Gorse, E. K. Heyerdahl, R. L. Johnson, J. A. Rau, and J. J. Huntzicker (1984), Comparison of solvent extraction and thermal-optical carbon analysis. Methods: Application to diesel vehicle exhaust aerosol, *Environ. Sci. Technol.*, *18*, 231–234.

Kasibhatla, P., A. Arellano, J. A. Logan, P. I. Palmer, and P. Novelli (2002), Top-down estimate of a large source of atmospheric carbon monoxide associated with fuel combustion in Asia, *Geophys. Res. Lett.*, *29*(19), 1900, doi:10.1029/2002GL015581.

Kaufman, Y. J., D. Tanre, and O. Boucher (2002), A satellite view of aerosols in the climate system, *Nature*, *419*, 215–223.

Keene, W. C., A. A. P. Pszenny, J. N. Galloway, and M. E. Hawley (1986), Sea-salt corrections and interpretation of constituent ratios in marine precipitation, *J. Geophys. Res.*, *91*, 6647–6658.

Kotchenruther, R. A., and P. V. Hobbs (1998), Humidification factors of aerosols from biomass burning in Brazil, *J. Geophys. Res.*, *103*, 32,081–32,089.

Luo, C., J. C. St. John, X. Zhou, K. S. Lam, T. Wang, and W. L. Chameides (2000), A nonurban ozone air pollution episode over eastern China: Observations and model simulations, *J. Geophys. Res.*, *105*, 1889–1908.

Ma, Y., et al. (2003), Characteristics and influence of biomass burning aerosols on fine particle ionic composition measured in Asian outflow during TRACE-P, *J. Geophys. Res.*, *108*(D21), 8816, doi:10.1029/2002JD003128.

Palmer, P., D. J. Jacob, D. B. A. Jones, C. L. Heald, R. M. Yantosca, J. Logan, G. Sachse, and D. Streets (2003), Inverting for emissions of carbon monoxide from Asia using aircraft observations over the western Pacific, *J. Geophys. Res.*, *108*(D21), 8828, doi:10.1029/2003JD003397.

Parrish, D. D., et al. (1993), The total reactive oxidized nitrogen levels and their partitioning between the individual species at six rural sites in eastern North America, *J. Geophys. Res.*, *98*, 2927–2939.

Parrish, D. D., M. Trainer, J. S. Holloway, J. E. Yee, M. S. Warshawsky, and F. C. Fehsenfeld (1998), Relationships between ozone and carbon monoxide at surface sites in the North Atlantic region, *J. Geophys. Res.*, *103*, 13,357–13,376.

Peng, Y., C. Luo, X. Xu, R. Xiang, G. Ding, J. Tang, M. Wang, and X. Yu (1997), The study of distribution character of O_3, NO_x and SO_2 at rural areas in China (in Chinese), *Q. J. Appl. Meteorol.*, *8*(1), 53–60.

Russo, R. S., et al. (2003), Chemical composition of Asian continental outflow over the western Pacific: Results from TRACE-P, *J. Geophys. Res.*, *108*(D20), 8804, doi:10.1029/2002JD003184.

Smyth, S., et al. (1999), Characterization of the chemical signatures of air masses observed during the PEM experiments over the western Pacific, *J. Geophys. Res.*, *104*, 16,243–16,254.

State Environmental Protection Administration (2002), *Report on the State of the Environment in China 2000*, Beijing.

Streets, D. G., and S. T. Waldhoff (2000), Present and future emissions of air pollutants in China: SO_2, NO_x, and CO, *Atmos. Environ.*, *34*, 363–374.

Streets, D. G., et al. (2003), An inventory of gaseous and primary aerosol emissions in Asia in the year 2000, *J. Geophys. Res.*, *108*(D21), 8809, doi:10.1029/2002JD003093.

Trainer, M., et al. (1993), Correlation of ozone with NO_y in photochemically aged air, *J. Geophys. Res.*, *98*, 2917–2925.

Van Aardenne, J., G. R. Carmichael, H. Levy II, D. Streets, and L. Hordijk (1999), Anthropogenic NO_x emissions in Asia in the period 1990–2020, *Atmos. Environ.*, *33*, 633–646.

Wang, C. J.-L., D. R. Blake, and F. S. Rowland (1995), Seasonal variations in the atmospheric distribution of a reactive chorine compound, tetrachloroethene ($CCl_2 = CCl_2$), *Geophys. Res. Lett.*, *22*, 1097–1110.

Wang, T., T. F. Cheung, M. Anson, and Y. S. Li (2001), Ozone and related gaseous pollutants in the boundary layer of eastern China: Overview of the recent measurements at a rural site, *Geophys. Res. Lett.*, *28*, 2373–2376.

Wang, T., T. F. Cheung, Y. S. Li, X. M. Yu, and D. R. Blake (2002), Emission characteristics of CO, NO_x, SO_2 and indications of biomass burning observed at a rural site in eastern China, *J. Geophys. Res.*, *107*(D12), 4157, doi:10.1029/2001JD000724.

Wang, T., A. J. Ding, D. R. Blake, W. Zahoroski, C. N. Poon, and Y. S. Li (2003), Chemical characterization of the boundary layer outflow of air pollution to Hong Kong during February–April 2001, *J. Geophys. Res.*, *108*(D20), 8787, doi:10.1029/2002JD003272.

Wang, W. X., and T. Wang (1995), On the origin and the trend of acid rain precipitation in China, *Water Air Soil Pollut.*, *85*, 2295–2300.

White, W. H., and P. T. Roberts (1977), On the nature and origins of visibility-reducing aerosols in the Los Angeles Air Basin, *Atmos. Environ.*, *11*, 803–812.

Xu, J., M. H. Bergin, X. Yu, G. Liu, J. Zhao, C. M. Carrico, and K. Baumann (2001), Measurement of aerosol chemical, physical and radiative properties in the Yangtze Delta region of China, *Atmos. Environ.*, *36*, 161–173.

Yao, X., C. K. Chan, M. Fang, S. Cadle, T. Chan, P. Mulawa, K. He, and B. Ye (2002), The water-soluble ionic composition of PM2.5 in Shanghai and Beijing, China, *Atmos. Environ.*, *36*, 4223–4234.

R. Arimoto, Environmental Monitoring and Research Center, New Mexico State University, 1400 University Drive, Carlsbad, NM 88220, USA. (arimoto@cemrc.org)

K. Baumann, School of Earth and Atmospheric Sciences, Georgia Institute of Technology, 221 Bobby Dodd Way, OCE 205, Atlanta, GA 30332-0340, USA. (kb@eas.gatech.edu)

D. R. Blake and I. J. Simpson, Department of Chemistry, University of California, Irvine, Rowland Hall, Irvine, CA 92697-2025, USA. (drblake@uci.edu; isimpson@uci.edu)

T. F. Cheung, Environment, Transport and Works Bureau (Environment Branch), 33/F, Revenue Tower, 5 Gloucester Road, Wanchai, Hong Kong, China. (vincent_tf_cheung@etwb.gov.hk)

G. A. Ding and J. Tang, Chinese Academy of Meteorological Sciences, Beijing 100081, China. (tangj@cams.cma.gov.cn)

Y. S. Li, T. Wang, and C. H. Wong, Department of Civil and Structural Engineering, Hong Kong Polytechnic University, Hung Hom, Kowloon, Hong Kong, China. (ceysli@polyu.edu.hk; cetwang@polyu.edu.hk)

D. G. Streets, Decision and Information Sciences Division, Argonne National Laboratory, DIS/900, 9700 South Cass Avenue, Argonne, IL 60439, USA. (dstreets@anl.gov)

X. M. Yu, Lin'an Baseline Air Pollution Monitoring Station, Zhejiang, China. (labams@la.hz.zj.cn)